Geophysical Research Letters

RESEARCH LETTER
10.1029/2025GL120811

Special Collection:
Land-atmosphere coupling: measurement, modelling and analysis

Changing Aerodynamic Roughness in WRF Reduces Bias and Improves Accuracy in Near-Surface Wind Simulations

Hongquan Song[1], Xueli Ni[1], Yujie Chang[1], Adrian Chappell[2], Zhuoli Zhou[3], and Boyan Liu[1]

[1]State Key Laboratory of Spatial Datum, Henan Key Laboratory of Air Pollution Control and Ecological Security, Faculty of Geographical Science and Engineering, Henan University, Zhengzhou, China, [2]School of Earth and Environmental Science, Cardiff University, Cardiff, UK, [3]State Key Laboratory of Earth Surface Processes and Resource Ecology, MOE Engineering Research Center of Desertification and Blown-Sand Control, Faculty of Geographical Science, Beijing Normal University, Beijing, China

Key Points:

- Changing aerodynamic roughness (CAR) improves the accuracy of near-surface wind simulation in WRF
- CAR reduces 10 m wind speed normalized mean bias from 14.6% to 2.2% and root mean square error from 0.5 to 0.3 m s^{-1} across China in 2023
- CAR yields large improvements over open surfaces, while improvements over closed canopies are more limited under skimming flow

Correspondence to:
H. Song and A. Chappell,
hqsong@henu.edu.cn;
chappella2@cardiff.ac.uk

Citation:
Song, H., Ni, X., Chang, Y., Chappell, A., Zhou, Z., & Liu, B. (2026). Changing aerodynamic roughness in WRF reduces bias and improves accuracy in near-surface wind simulations. *Geophysical Research Letters*, *53*, e2025GL120811. https://doi.org/10.1029/2025GL120811

Received 26 NOV 2025
Accepted 17 FEB 2026

Author Contributions:
Conceptualization: Hongquan Song, Adrian Chappell
Formal analysis: Hongquan Song, Xueli Ni
Funding acquisition: Hongquan Song
Investigation: Hongquan Song, Xueli Ni, Yujie Chang, Adrian Chappell, Zhuoli Zhou, Boyan Liu
Methodology: Hongquan Song, Xueli Ni, Yujie Chang, Adrian Chappell
Project administration: Hongquan Song
Resources: Xueli Ni, Yujie Chang
Software: Xueli Ni, Yujie Chang
Supervision: Hongquan Song
Validation: Xueli Ni, Yujie Chang

Abstract Accurate simulation of near-surface wind speed is crucial for applications in renewable energy, dust emission, and air quality modeling. However, the Weather Research and Forecasting (WRF) model systematically over-estimates 10 m wind speed due to simplified representations of surface roughness and momentum exchange. Here we incorporate into WRF a physically based changing aerodynamic roughness (CAR) scheme using satellite albedo, to dynamically adjust near-surface wind friction and momentum exchange. Simulations during 2023 over China show that CAR substantially improves near-surface wind speed estimates, reducing the normalized mean bias from 14.6% to 2.2%. The improvements are pronounced over cropland, shrubland, grassland, and bare land. Limited improvements occur in closed canopies (forests and urban areas) because CAR poorly represents skimming flow. Nevertheless, bridging satellite observations with boundary-layer dynamics, the CAR scheme provides a more realistic representation of surface–atmosphere momentum exchange, offering enhanced reliability for climate, air-quality, and wind-resource studies.

Plain Language Summary Accurate near-surface wind simulations are essential for weather forecasting, air-quality assessment, dust-storm prediction, and wind-energy planning. However, most climate models show substantial bias in simulating near-surface wind speeds because they rely on fixed and overly simplified aerodynamic roughness that cannot represent continuous changes in land surface conditions. In this study, we introduce a Changing Aerodynamic Roughness (CAR) scheme into the Weather Research and Forecasting (WRF) model, using satellite observations to link wind friction to real variations in land-surface properties. By dynamically adjusting surface roughness in response to changes in vegetation cover, soil texture, and land use, CAR provides a realistic representation of surface-atmosphere interactions. Applied to simulations over China in 2023, CAR substantially improved the agreement between modeled and observed winds. The mean bias in 10-m wind speed decreased from 14.6% to 2.2%, with consistent improvements across seasons, particularly over cropland, shrubland, grassland, and bare land. This approach produces more physically realistic wind fields to enhance applications such as air-quality modeling, dust-emission prediction, and wind-energy assessment.

1. Introduction

Accurate simulation of near-surface wind speed is essential for applications ranging from wind energy assessment and air pollution dispersion to dust storm prediction and climate risk management (Allen et al., 2017; Dent et al., 2021; Menut, 2018; Paulot et al., 2022). Wind speed, typically at 10 m above ground level (U_{10}), is a key variable in numerical weather prediction (NWP) and regional climate simulations (Gilliam et al., 2015; Wagenbrenner et al., 2016). It directly influences surface momentum exchange, turbulent mixing, and the transport of heat, moisture, and aerosols. Despite advances in model physics and computing power, mesoscale models such as the Weather Research and Forecasting (WRF) model still exhibit persistent biases in near-surface wind simulations across diverse terrain and land cover types (Bianco et al., 2019; Horvath et al., 2012; Nelli et al., 2020). These biases arise from multiple interacting factors related to both model physics and surface representation. Inaccuracies in planetary boundary layer (PBL) schemes, surface layer formulations, and land surface models (LSMs) can misrepresent turbulence, stability, and surface–atmosphere momentum transfer, particularly under stable boundary layers and in complex terrain (Bianco et al., 2019; Carvalho et al., 2012;

Visualization: Adrian Chappell, Zhuoli Zhou, Boyan Liu
Writing – original draft: Hongquan Song
Writing – review & editing: Xueli Ni, Yujie Chang, Adrian Chappell, Zhuoli Zhou, Boyan Liu

Moraes et al., 2005; Prieto-Herráez et al., 2021). While sensitivity experiments have identified optimal combinations of physics schemes, residual biases often remain (Díaz-Isaac et al., 2018; Prein et al., 2022), highlighting the need for more physically based parameterizations for further improve near-surface wind simulations.

A major contributor to wind speed errors is the reliance on static aerodynamic roughness length (z_0) fields, fixed over space derived from generalized land-use/land cover categories and static over time (Li et al., 2023; Nelli et al., 2020). Since z_0 and friction velocity (u_*) constrain the vertical wind profile, fixed values in those parameters neglect sub-grid scale variability (heterogeneity within a land use/land cover class) driven by slow changes like seasonality, vegetation phenology, agricultural practices, and more abrupt changes in land-use, snow cover, and fires. Static parameterizations can cause large wind biases in small roughness areas and seasonal wind speed errors linked to vegetation state (Wang et al., 2019; Yu et al., 2022). For example, in hyper-arid regions, observed z_0 values are often an order of magnitude smaller than WRF defaults, leading to systematic under-estimation of U_{10}, with errors substantially reduced when more representative values are applied (Nelli et al., 2020). Recent efforts to improve z_0 representation include satellite-based retrievals (Liu et al., 2023), roughness sublayer parameterizations (Lee et al., 2020), and urban canopy refinements (Wang et al., 2025), though these approaches often remain region-specific.

Beyond these broad limitations, certain physical processes are represented with insufficient detail, producing localized but significant wind speed errors. Targeted corrections for such processes can yield notable local improvements but are generally difficult to make universal (across regions and applications). In parallel, a variety of statistical and machine learning methods have been developed, including sequence transfer (Wang et al., 2019), hybrid deep learning frameworks (Han et al., 2022), surrogate optimization (Di et al., 2019), and neural network bias correction (Adomako et al., 2024; Xu et al., 2025). While these methods can reduce mean errors, they rely heavily on high-quality historical observations (Han et al., 2022; Wang et al., 2019; Xu et al., 2025). Such data-driven correction schemes often exhibit limited physical interpretability, as they primarily focus on empirical bias reduction without addressing the underlying physical origins of error, and consequently show poor transferability to data-sparse regions (Adomako et al., 2024; Di et al., 2019).

In this study, we developed a correction framework combined with an empirical formulation proposed by Chappell and Webb (2016), in which u_* is normalized by the wind velocity (U) at the freestream height $f(U_f)$. The normalization factor (u_*/U_f) was directly derived from satellite-retrieved albedo, providing a dynamic aerodynamic roughness (not length scale) (Zhou et al., 2024) that represents spatio-temporal variations in surface conditions. By linking the wind profile at 10 m with that at a freestream height, we derived a modified model that corrects WRF-simulated U_{10}. This correction framework has been fully coupled into WRF version 4.1.1, ensuring that the dynamic surface information from remote sensing is embedded in WRF wind simulations. Here we show that this novel, physically based and universal approach to improving near-surface wind simulations, offers new insights for wind energy assessment, dust emission modeling, and land–atmosphere interaction studies.

2. Material and Methods

2.1. Changing Aerodynamic Roughness (CAR) Derived From Remote Sensing Observations

The coupling between land surface wind friction and the freestream flow can be quantified by the friction velocity normalized by the freestream wind speed (u_*/U_f). Building on the relation between shadow and shelter established by Raupach (1992), Chappell and Webb (2016) developed an albedo-based relation linking the proportion of surface shadow, including mutual shadowing effects, to the aerodynamic properties of the land surface. The normalized and rescaled surface shadow (ω_{ns}) provides a quantitative indicator of surface roughness derived from satellite observations (Chappell et al., 2018; Chappell & Webb, 2016). The normalized shadow is defined as:

$$\omega_n = \frac{1 - \omega_{\mathrm{dir}}(0^\circ)}{f_{\mathrm{iso}}} \tag{1}$$

where $\omega_{\mathrm{dir}}(0^\circ)$ is the directional albedo at a solar zenith angle of 0°, and f_{iso} is the isotropic bidirectional reflectance distribution function (BRDF) parameter from the MODIS BRDF-albedo model (MCD43A1.061). This term corrects spectral variations associated with soil composition, organic carbon, and moisture. The normalized shadow is then rescaled from the numerical simulations to the MODIS values and calculated as:

$$\omega_{ns} = (a - b)\frac{(\omega_n - \omega_{n,\max})}{(\omega_{n,\min} - \omega_{n,\max})} + b \tag{2}$$

where $a = 0.0001$, $b = 0.1$, $\omega_{n,\min} = 0$, and $\omega_{n,\max} = 35$. Building on this concept, the u_*/U_f can be expressed empirically as a function of ω_{ns} (Chappell & Webb, 2016):

$$\mathrm{CAR} = \frac{u_*}{U_f} = 0.0497\left(1 - \exp\left(-\frac{\omega_{ns}^{1.326}}{0.0027}\right)\right) + 0.038 \tag{3}$$

This formulation removes the direct influence of wind magnitude and isolates the effect of surface roughness, represented by the satellite-derived shadow proportion, on surface momentum exchange. For convenience, we define the ratio u_*/U_f as the changing aerodynamic roughness (CAR). Atmospheric stability effects are explicitly handled by the WRF surface-layer scheme, and CAR is therefore formulated to modulate roughness-related momentum extraction without introducing an additional stability dependence.

The CAR serves as a dimensionless indicator of surface–atmosphere coupling strength and is not intended to represent a retrieval or redefinition of the classical aerodynamic roughness length z_0. Instead, it represents an effective measure of aerodynamic roughness based on momentum extraction efficiency (u_*/U_f), describing the integrated influence of surface roughness elements on near-surface flow. The CAR is grounded in aerodynamic turbulence theory and calibrated against friction velocity u_* using experimentally derived relationships between surface structure and momentum extraction, with its physical validity supported by independent field-based studies (Chappell & Webb, 2016; Raupach, 1992; Zhou et al., 2024). Larger CAR values correspond to rougher or more vegetated surfaces with stronger wind friction and energy dissipation, whereas smaller values indicate smoother or bare surfaces with weaker coupling. By varying dynamically with satellite-observed surface conditions, CAR captures spatio-temporal variability in aerodynamic effects that are not represented by the static roughness formulation in the default WRF model.

2.2. Derivation of the Corrected 10 m Wind Speed

In the WRF model, near-surface wind speed is diagnosed with the logarithmic wind profile based on Monin-Obukhov similarity theory (Jiménez et al., 2012). Under neutral atmospheric conditions, the mean wind speed at height z is expressed as:

$$U_z = \frac{u_*}{k}\ln\left(\frac{z}{z_0}\right) \tag{4}$$

where u_* is the friction velocity, $k = 0.4$ is the von Kármán constant, and z_0 is the aerodynamic roughness length. Based on the logarithmic wind profile, U_f and U_{10} can be expressed as:

$$U_f = \frac{u_*}{k}\ln\left(\frac{f}{z_0}\right) \tag{5}$$

$$U_{10} = \frac{u_*}{k}\ln\left(\frac{10}{z_0}\right) \tag{6}$$

Eliminating u_*, U_f can be calculated from U_{10}:

$$U_f = U_{10}\frac{\ln\left(\frac{f}{z_0}\right)}{\ln\left(\frac{10}{z_0}\right)} \tag{7}$$

Subtracting U_f from U_{10} yields:

$$U_{10} = U_f + \frac{u_*}{k}\ln\left(\frac{10}{f}\right) \tag{8}$$

This expression explicitly links U_{10} to u_* and U_f. Based on the relationship between CAR and u_*/U_f in Equation 3, the CAR-corrected U_{10} can be redefined as:

$$U_{10}^c = U_f\left[1 + \frac{CAR}{k}\ln\left(\frac{10}{f}\right)\right] \tag{9}$$

Replacing U_f with U_{10} in Equation 7:

$$U_{10}^c = U_{10}\frac{\ln\left(\frac{f}{z_0}\right)}{\ln\left(\frac{10}{z_0}\right)}\left[1 + \frac{\mathrm{CAR}}{k}\ln\left(\frac{10}{f}\right)\right] \tag{10}$$

Therefore, the corrected 10 m wind speed output by the WRF model can be rewritten as:

$$WU_{10}^c = WU_{10}\frac{\ln\left(\frac{f}{Wz_0}\right)}{\ln\left(\frac{10}{Wz_0}\right)}\left[1 + \frac{CAR}{k}\ln\left(\frac{10}{f}\right)\right] \tag{11}$$

where WU_{10}^c denotes the corrected 10 m wind speed for WRF, WU_{10} is the 10 m wind speed simulated by the original WRF model, and Wz_0 represents the fixed aerodynamic roughness length prescribed in WRF. Here, CAR is applied in a post-processing framework to isolate the effect of aerodynamic roughness variability on near-surface wind speed. We adopt a fixed freestream height of $f = 100$ m, which provides a consistent reference level for evaluating the surface-flow coupling in the surface layer.

2.3. Integration of the CAR Parameterization Into WRF

The CAR parameterization was integrated into WRF (version 4.1.1) to enable real-time adjustment of near-surface wind speed based on satellite remote-sensing observations of surface conditions. This integration allowed the simulated 10 m wind to respond dynamically to spatio-temporal variations in land-surface aerodynamic properties while maintaining the internal physical consistency of the model. Daily CAR data, derived from MODIS albedo products, were re-gridded and re-projected to match the WRF computational domain and temporal resolution. The resulting CAR field was stored in NetCDF format that WRF could read as an external variable. During runtime, the surface layer driver was modified to import the dynamic CAR field at each time step.

The integration was designed as an online diagnostic correction which modifies only the diagnosed 10 m wind without affecting the model's prognostic momentum fluxes, turbulence, or boundary-layer tendencies. Consequently, the new parameterization remains compatible with WRF's PBL schemes while improving the realism of near-surface wind representation. Through this integration, WRF gains the capability to represent the dynamic influence of surface roughness on near-surface wind speeds, bridging satellite-derived surface observations with boundary-layer dynamics.

2.4. Model Setup and Experimental Design

To evaluate the performance of the dynamic CAR parameterization, the WRF model was configured over a domain containing China, covering a wide range of surface conditions. The model domain employed a Lambert conformal projection centered at 36.5°N, 102.2°E, with a horizontal resolution of 25 km and 28 vertical levels extending from the surface to 100 hPa. The initial and lateral boundary conditions were obtained from the National Centers for Environmental Prediction (NCEP) Final Analysis (FNL) data at 1° × 1° spatial and 6-hourly temporal resolution (DOC/NOAA/NWS/NCEP). The physical parameterizations employed in this study included the Yonsei University (YSU) scheme for the PBL, the Unified Noah land surface model, the Goddard shortwave and longwave radiation schemes, the Purdue Lin microphysics scheme, and the Betts-Miller-Janjic (BMJ) ensemble cumulus parameterization.

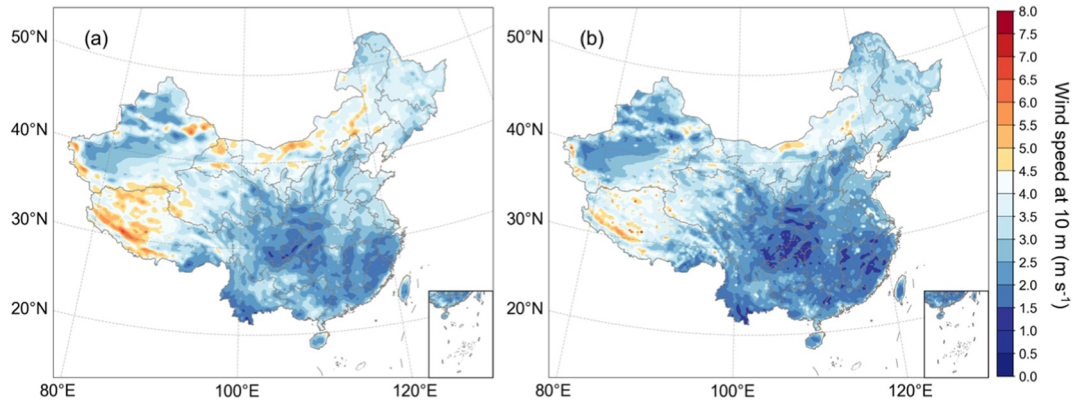

Figure 1. Spatial distributions of annual mean 10 m wind speed (m s^{-1}) over China in 2023 simulated by the original WRF configuration Exp-CTL (a) and the modified WRF model incorporating the changing aerodynamic roughness (CAR) parameterization Exp-CAR (b).

Two sets of experiments were conducted to isolate the effects of the dynamic CAR correction. The control simulation (Exp-CTL) followed the standard WRF configuration, in which 10 m wind speeds were diagnosed based on static z_0 values derived from the land cover lookup table. In contrast, the dynamic experiment (Exp-CAR) activated the newly integrated CAR module, where the spatially and temporally varying CAR field provided observation-informed corrections to the diagnosed 10 m wind speeds. Both experiments were driven by identical meteorological boundary conditions and land cover data to ensure consistent forcing and allow direct comparison of near-surface wind performance. The simulations covered the full year of 2023, with an additional 7-day spin-up period at the beginning of the simulation to minimize the influence of initial conditions. The comparison between simulations with and without CAR is designed to isolate the role of aerodynamic roughness representation, rather than to eliminate all sources of uncertainty inherent in regional climate modeling.

Satelite albedo data were obtained from the MODIS (MCD43A1 V6.1 BRDF) product, which provides isotropic parameters at 500 m spatial resolution and daily temporal resolution (Schaaf & Wang, 2021). Model evaluation was performed using wind speed observations sampled at hourly temporal resolution from 404 surface meteorological stations distributed across China, obtained from the Integrated Surface Database (ISD-Lite) provided by the U.S. National Centers for Environmental Information (NCEI). Model performance was evaluated using the Mean Bias (MB), Normalized Mean Bias (NMB), Normalized Mean Error (NME), Root Mean Square Error (RMSE), and Correlation Coefficient (R), with all metrics calculated following the definitions in Song et al. (2017). This evaluation framework provides a robust basis for quantifying improvements in near-surface wind simulations achieved through the incorporation of the dynamic CAR parameterization and for examining its regional dependence across different land surface conditions.

3. Results

3.1. Spatial Distribution of Simulated Wind Speed Experiments

Figure 1 shows the spatial distributions of annual mean U_{10} over China in 2023 simulated by the Exp-CTL and Exp-CAR. Both simulations capture the large-scale climatological gradient of U_{10} across China, featuring a gradual increase from the humid southeast toward the arid northwest. Large wind speeds occur mainly over arid and sparsely vegetated regions with open terrain, while smaller values dominate the southeastern and southwestern areas, where complex topography and dense vegetation increase surface wind friction and weaken near-surface flow. Although the overall spatial structures are broadly consistent between the two simulations, noticeable differences emerge after the incorporation of the CAR scheme. Compared with Exp-CTL (Figure 1a), the Exp-CAR (Figure 1b) simulation generally produces smaller U_{10} across most regions, particularly over areas with pronounced land surface heterogeneity.

The inclusion of CAR allows effective aerodynamic roughness to vary daily in response to local surface conditions, resulting in systematic adjustments of near-surface wind speed across most regions. Reductions in U_{10} are most pronounced in areas where Exp-CTL exhibits relatively large wind speeds, leading to an expansion of small

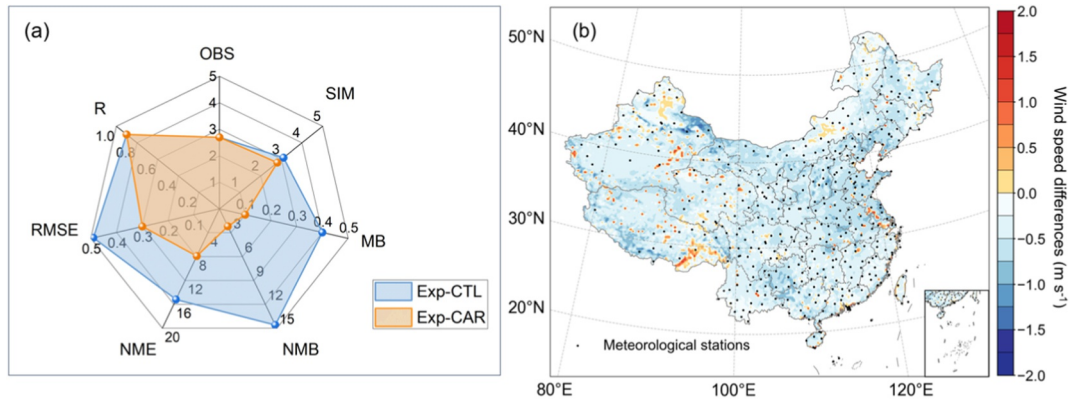

Figure 2. (a) Comparison of statistical metrics for 10 m wind speed between the Exp-CTL and Exp-CAR experiments, including station-averaged observed mean (m s^{-1}), simulated mean (m s^{-1}), MB (m s^{-1}), NMB(%), NME (%), RMSE (m s^{-1}) and R. (b) Spatial distribution of the annual mean difference in 10 m wind speed (Exp-CAR minus Exp-CTL) over China in 2023, with black dots indicating meteorological observation stations.

wind-speed areas and a substantial suppression of large near-surface winds. Overall, Exp-CAR produces more extensive regions of small wind speeds and markedly reduces the unrealistically large wind speeds evident in Exp-CTL.

3.2. Performance of the WRF Model With the CAR Scheme

The statistical evaluation of simulations (SIM) against observed 10 m wind speed (OBS) reveals that the incorporation of the CAR scheme substantially improves the near-surface wind simulation (Figure 2a). The mean OBS across all meteorological stations was 2.7 m s^{-1}, whereas the SIM mean from Exp-CTL was 3.1 m s^{-1}, showing a clear positive bias. In Exp-CAR, the SIM mean wind speed decreases to 2.8 m s^{-1}, closer to the observations. Similarly, the mean bias (MB = SIM − OBS) of 0.4 m s^{-1} in Exp-CTL, decreased to 0.1 m s^{-1} in Exp-CAR. Both NMB and NME decreased substantially, from 14.6% and 15.2% in Ext-CTL to 2.2% and 7.9% in Exp-CAR, respectively. The RMSE reduced from 0.5 to 0.3 m s^{-1}, comparing the two simulations. The correlation coefficient R between SIM and OBS winds remained nearly unchanged at a consistently large value of 0.9, indicating stable temporal agreement. These results clearly demonstrate that Exp-CAR effectively mitigated the systematic over-estimation of 10 m wind speed and enhanced the overall performance of the model.

The annual mean difference in U_{10} (Exp-CAR minus Exp-CTL) exhibited a coherent pattern across China (Figure 2b). The U_{10} differences between the two scenarios are predominantly negative across most regions of China, indicating that the integration of the CAR scheme generally reduced near-surface wind speeds compared with the original WRF simulation. The magnitude of this reduction typically ranges from −1 to 0 m s^{-1}, with larger decreases exceeding −1 m s^{-1} in localized areas, particularly in northwestern China. In contrast, small positive differences (>0.5 m s^{-1}) occur in some high-altitude or densely vegetated regions, suggesting a limited local enhancement of near-surface wind speed associated with the CAR scheme. By changing aerodynamic roughness in response to local land surface conditions and particularly vegetation structure, the CAR scheme enhanced surface drag and momentum dissipation, thereby reduced the systematic over-estimation of wind speed and improved the spatial realism of wind fields.

3.3. Monthly Variations of Model Performance

The monthly variations of NMB relative to observed 10 m wind speed showed that the incorporation of the CAR scheme systematically improves the U_{10} simulation throughout the year (Figure 3). In Exp-CTL, NMB remained positive during all months, ranging from 4.87% in August to 21.09% in January, indicating a consistent over-estimation of near-surface winds. In contrast, Exp-CAR substantially reduced this bias, with NMB values varying between −6.6% in August and 13.62% in January. The largest reductions occur during spring (March–May), when the monthly NMB decreased by approximately 15%–18% compared with Exp-CTL. The inclusion of CAR markedly reduced the month-to-month variability of NMB, moderating excessive seasonal oscillations, and yielding a more consistent simulation of near-surface winds. These results demonstrate that dynamically

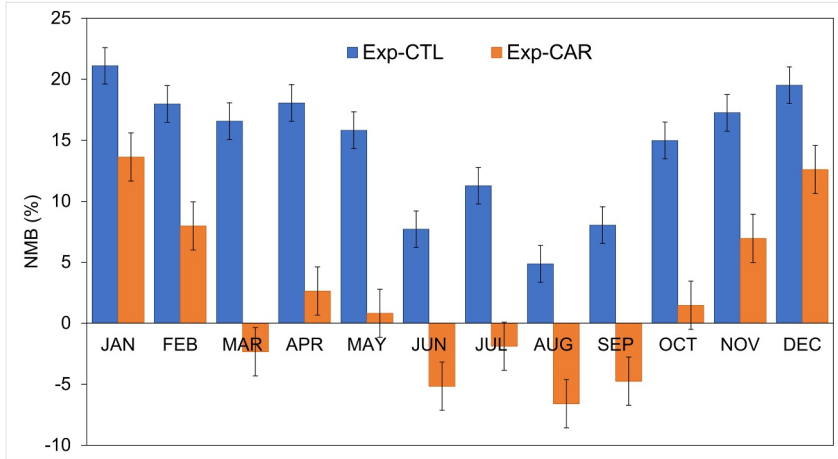

Figure 3. Monthly variations of the normalized mean bias (NMB) of simulated 10 m wind speed over China in 2023 for the Exp-CTL and Exp-CAR experiments. Error bars indicate the standard deviations of NMB across all meteorological stations.

representing surface roughness not only corrects the systematic large bias but also improves the seasonal stability of near-surface wind simulations.

Seasonal variations showed that the most pronounced improvements occurred in spring (March–May), followed by autumn (September–November), when the differences between Exp-CTL and Exp-CAR are the largest. During summer (June–August), simulated wind speeds in Exp-CAR become slightly under-estimated relative to observations but overall remain much closer to the measured values than those from Exp-CTL. In winter (December–February), although the improvement was smaller compared with other seasons, Exp-CAR still exhibited a substantial reduction in NMB, indicating that the systematic large bias is effectively mitigated throughout the year. Overall, the CAR scheme reduces wind-speed over-estimation in all months, with the most pronounced differences appearing during transitional seasons between the two simulations.

3.4. Model Performance Across Different Land-Cover Types

Table 1 summarizes the model performance for simulated U_{10} over six representative land cover types. In the Exp-CTL experiment, the WRF model generally over-estimates near-surface wind speeds across all surface categories, with positive NMB values ranging from 4.59% (forests) to 22.11% (croplands). The MB varied

Table 1
Comparison of the Performance of Simulated 10 m Wind Speed for Different Land-Cover Types Between the Exp-CTL and Exp-CAR Experiments

Land-cover type	Experiment	Observation (m s^{-1})	Simulation (m s^{-1})	MB (m s^{-1})	NMB (%)
Forests	Exp-CTL	2.29	2.39	0.10	4.59
	Exp-CAR		2.18	−0.11	−4.84
Shrublands	Exp-CTL	3.01	3.68	0.67	22.09
	Exp-CAR		3.11	0.09	3.11
Grasslands	Exp-CTL	2.72	3.09	0.37	13.74
	Exp-CAR		2.73	0.01	0.03
Croplands	Exp-CTL	2.49	3.05	0.55	22.11
	Exp-CAR		2.53	0.04	1.41
Urban areas	Exp-CTL	2.96	3.24	0.28	9.31
	Exp-CAR		3.17	0.20	6.86
Bare lands	Exp-CTL	3.01	3.53	0.52	17.08
	Exp-CAR		3.08	0.06	2.11

between 0.10 and 0.67 m s^{-1}, indicating a large bias independent of surface types. After implementing the CAR scheme, these over-estimations were substantially reduced. The NMB values for most surfaces approach zero or become slightly negative, ranging between −4.84% and 6.86%. The improvement is most notable over grasslands, croplands, shrublands, and bare lands regions, where simulated wind speeds were reduced by around 0.4–0.6 m s^{-1} compared with Exp-CTL. Although Exp-CAR still over-estimates U_{10} in urban areas, the CAR scheme reduces the magnitude of positive bias, though with limited improvement. Specifically, the MB decreases from 0.28 to 0.20 m s^{-1}, and the NMB declines from 9.31% to 6.86%. In contrast, over forested regions characterized by high surface roughness and pronounced subgrid-scale heterogeneity, the application of CAR leads to an overcorrection, with the bias changing sign from positive to negative. The Exp-CTL simulation exhibits a slight over-estimation (MB = 0.10 m s^{-1}; NMB = 4.59%), whereas Exp-CAR produces a mild under-estimation (MB = −0.11 m s^{-1}; NMB = −4.84%).

The contrasting behavior among land-cover types represented the physical mechanism of the CAR parameterization. By linking changing aerodynamic roughness to land surface heterogeneity and vegetation structure, the scheme enhances surface wind friction where land surface features or canopy elements intensify momentum dissipation. Over croplands and shrublands, seasonal changes in vegetation height and density strongly affect aerodynamic roughness. The CAR represents these variations as they change over time, preventing the over-estimation of wind speeds that occurs when z_0 values are fixed over large classes and static over time. Over bare or sparsely vegetated lands, the scheme moderates the unrealistic acceleration of near-surface flow by representing roughness induced by soil roughness and micro-topography. In contrast, over dense forest and urban surfaces, where the effective roughness is already large, the CAR-induced corrections are smaller but still beneficial in reducing residual large-bias events. Overall, the land cover-specific analysis confirms that the CAR scheme effectively adapts to diverse surface environments and provides a more physically realistic depiction of land–atmosphere momentum exchange across heterogeneous landscapes.

4. Discussion and Conclusion

The incorporation of a physically based CAR scheme into the WRF model substantially improves the simulation of near-surface wind speed. The WRF model with the CAR scheme effectively reduces the systematic large bias that is common in the standard model, decreases RMSE and NMB by nearly half, and yields a stronger temporal correlation with observations. The most pronounced improvements occur in spring and autumn, when surface conditions vary rapidly, and across grasslands, croplands, shrublands, and bare-lands surfaces where static roughness parameterizations perform poorly. Overall, the CAR implementation provides a more balanced and physically consistent representation of near-surface winds, offering a reliable foundation for applications such as air-quality modeling, dust-emission estimation, and wind-energy assessment.

The overall improvements of near-surface wind simulations arise primarily from the enhanced representation of surface wind friction and momentum dissipation. The original WRF configuration always over-estimates wind speeds because values of z_0 are fixed over large spatial classes and are static over time which under-estimates the true surface resistance, particularly in heterogeneous or vegetated landscapes (Jiménez & Dudhia, 2012; Nelli et al., 2020; Shen et al., 2022; Wang et al., 2025). By introducing a relation between aerodynamic roughness and local land surface conditions, the CAR scheme strengthens frictional coupling in the surface layer and prevents the excessive downward transport of momentum. Consequently, near-surface winds are weakened where the default model previously produced unrealistically strong flows, leading to a more physically realistic wind field that better aligns with the observed climatological gradient. This overall pattern of the difference between Exp-CTL and Exp-CAR (Figure 2b) is consistent with previous evaluations of WRF wind simulations, which have reported widespread over-estimation of 10 m wind speed due to over-simplified roughness parameterizations (Falasca et al., 2021; Gholami et al., 2021; Jiménez & Dudhia, 2012; Yu et al., 2022).

The inclusion of CAR improves the temporal consistency of simulated winds and obviously suppresses the month-to-month variability of model bias. The largest corrections occur in spring and autumn, when rapid transitions in vegetation and soil conditions strongly modify surface roughness and boundary-layer turbulence. Although the default WRF assigns two fixed z_0 values for summer and winter to represent seasonal contrasts, this static treatment cannot represent the continuous sub-seasonal variability in surface properties (Shen et al., 2022; Vautard et al., 2010). The dynamically adjusted CAR scheme responds to evolving surface states, yielding significant improvements in all seasons. In summer, enhanced canopy wind friction and vigorous turbulent

mixing constrain roughness variation (Maurer et al., 2013) but still lead to clear bias reduction. While in winter, reduced vegetation limits the magnitude of surface change, yet small-scale roughness effects are better resolved. Overall, CAR complements the seasonal z_0 approach by continuously adapting to land-surface dynamics, producing more consistent and physically realistic near-surface winds throughout the year.

The contrasting responses among land-cover types reveal the underlying physical mechanisms of the CAR parameterization. By linking changing aerodynamic roughness to local land surface heterogeneity and vegetation structure, the scheme enhances surface wind friction where terrain features or canopy elements intensify momentum dissipation. Over croplands and shrublands, seasonal changes in vegetation height and density strongly affect aerodynamic roughness. The CAR scheme represents these changes over time, preventing the overestimation of wind speeds that occur when static z_0 values are applied. Over bare or sparsely vegetated areas, it moderates the unrealistic acceleration of near-surface flow by accounting for roughness induced by soil texture and micro-topography.

Over highly heterogeneous and rough surfaces, several factors may contribute to wind speed over-correction in forests and more limited improvement in urban areas. First, uncertainties in CAR derived from MODIS albedo products may be amplified by mixed pixels and anisotropic reflectance effects over heterogeneous land covers, affecting the robustness of the correction. Second, the assumption that the 10 m level lies within the inertial sublayer may be violated in environments characterized by canopy- or building-induced drag and elevated roughness sublayers, reducing the sensitivity of near-surface wind to changes in effective aerodynamic roughness. Third, over high-roughness surfaces, the effective freestream height may exceed the fixed value of 100 m adopted in this study, implying a land-cover dependence that can influence the magnitude of wind speed adjustment.

These methodological and representational limitations are consistent with well-established aerodynamic theory over dense canopies, which provides a physical basis for the observed behavior. The limited improvement over forests and urban areas is most likely explained by the parameterization of Raupach's (1992) drag partition framework. This framework showed that as roughness density increases, the ratio of friction velocity to canopy-top wind first rises with increasing form drag, then declines once canopies become closed. In this drag saturated regime, momentum exchange is dominated by canopy or building form drag, and additional roughness no longer enhances total stress. The flow above dense canopies transitions to skimming flow, in which near-surface wind becomes insensitive to further increases in surface wind friction. However, the CAR formulation follows the original parameterization and does not explicitly account for this curvilinear reduction of coupling at large roughness densities (Chappell & Webb, 2016). Consequently, its fractional correction may overcompensate surface resistance in closed canopies such as forests and cities, leading to the slight under-estimation of wind speed observed in these regions.

Conflict of Interest

The authors declare no conflicts of interest relevant to this study.

Data Availability Statement

The WRF (v4.1.1) model code is available from the official WRF repository (https://github.com/wrf-model/WRF/releases?page=3). All modified WRF codes developed in this study have been archived in Figshare (Song et al., 2025). The FNL reanalysis data were obtained from the NCAR RDA (DOC/NOAA/NWS/NCEP, 2000). The MCD43A1 V6.1 BRDF/Albedo data is publicly available and can be accessed via Google Earth Engine (https://developers.google.com/earth-engine/datasets/catalog/MODIS_061_MCD43A1). Observational 10 m wind speed data used in this study are from the Integrated Surface Data-Lite (ISD-Lite) dataset, accessible at https://www.ncei.noaa.gov/pub/data/noaa/isd-lite.

Acknowledgments
This work is supported by the Natural Science Foundation of Henan Province (242300421143), the Science and Technology Innovation Talents in Universities of Henan Province (24HASTIT016), and the National Natural Science Foundation of China (32130066).

References

Adomako, A. B., Jamshidi, E. J., Yusup, Y., Elsebakhi, E., Jaafar, M. H., Ishak, M. I. S., et al. (2024). Deep learning approaches for bias correction in WRF model outputs for enhanced solar and wind energy estimation: A case study in East and West Malaysia. *Ecological Informatics*, *84*, 102898. https://doi.org/10.1016/j.ecoinf.2024.102898

Allen, D. J., Tomlin, A. S., Bale, C. S. E., Skea, A., Vosper, S., & Gallani, M. L. (2017). A boundary layer scaling technique for estimating near-surface wind energy using numerical weather prediction and wind map data. *Applied nergy*, *208*, 1246–1257. https://doi.org/10.1016/j.apenergy.2017.09.029

Bianco, L., Djalalova, I. V., Wilczak, J. M., Olson, J. B., Kenyon, J. S., Choukulkar, A., et al. (2019). Impact of model improvements on 80 m wind speeds during the second Wind Forecast Improvement Project (WFIP2). *Geoscientific Model Development*, *12*(11), 4803–4821. https://doi.org/10.5194/gmd-12-4803-2019

Carvalho, D., Rocha, A., Gómez-Gesteira, M., & Santos, C. (2012). A sensitivity study of the WRF model in wind simulation for an area of high wind energy. *Environmental Modelling and Software*, *33*, 23–34. https://doi.org/10.1016/j.envsoft.2012.01.019

Chappell, A., & Webb, N. P. (2016). Using albedo to reform wind erosion modelling, mapping and monitoring. *Aeolian Research*, *23*, 63–78. https://doi.org/10.1016/j.aeolia.2016.09.006

Chappell, A., Webb, N. P., Guerschman, J. P., Thomas, D. T., Mata, G., Handcock, R. N., et al. (2018). Improving ground cover monitoring for wind erosion assessment using MODIS BRDF parameters. *Remote Sensing of Environment*, *204*, 756–768. https://doi.org/10.1016/j.rse.2017.09.026

Deng, K., Azorin-Molina, C., Minola, L., Zhang, G., & Chen, D. (2021). Global near-surface wind speed changes over the last decades revealed by reanalyses and CMIP6 model simulations. *Journal of Climate*, *34*(6), 2219–2234. https://doi.org/10.1175/jcli-d-20-0310.1

Di, Z., Ao, J., Duan, Q., Wang, J., Gong, W., Shen, C., et al. (2019). Improving WRF model turbine-height wind-speed forecasting using a surrogate-based automatic optimization method. *Atmospheric Research*, *226*, 1–16. https://doi.org/10.1016/j.atmosres.2019.04.011

Díaz-Isaac, L., Lauvaux, T., & Davis, K. (2018). Impact of physical parameterizations and initial conditions on simulated atmospheric transport and CO_2 mole fractions in the US Midwest. *Atmospheric Chemistry and Physics*, *18*(20), 14813–14835. https://doi.org/10.5194/acp-18-14813-2018

DOC/NOAA/NWS/NCEP National Centers for Environmental Prediction, National Weather Service, NOAA, U.S. Department of Commerce. (2000). NCEP FNL operational model global tropospheric analyses, continuing from July 1999 [Dataset]. *NSF National Center for Atmospheric Research*. https://doi.org/10.5065/D6M043C6

Falasca, S., Gandolfi, I., Argentini, S., Barnaba, F., Casasanta, G., Liberto, D. I., et al. (2021). Sensitivity of near-surface meteorology to PBL schemes in WRF simulations in a port-industrial area with complex terrain. *Atmospheric Research*, *264*, 105824. https://doi.org/10.1016/j.atmosres.2021.105824

Gholami, S., Ghader, S., Khaleghi-Zavareh, H., & Ghafarian, P. (2021). Sensitivity of WRF-simulated 10 m wind over the Persian Gulf to different boundary conditions and PBL parameterization schemes. *Atmospheric Research*, *247*, 105147. https://doi.org/10.1016/j.atmosres.2020.105147

Gilliam, R. C., Hogrefe, C., Godowitch, J. M., Napelenok, S., Mathur, R., & Rao, S. T. (2015). Impact of inherent meteorology uncertainty on air quality model predictions. *Journal of Geophysical Research: Atmospheres*, *120*(23), 12–259. https://doi.org/10.1002/2015jd023674

Han, Y., Mi, L., Shen, L., Cai, C. S., Liu, Y., Li, K., & Xu, G. (2022). A short-term wind speed prediction method utilizing novel hybrid deep learning algorithms to correct numerical weather forecasting. *Applied Energy*, *312*, 118777. https://doi.org/10.1016/j.apenergy.2022.118777

Horvath, K., Koracin, D., Vellore, R., Jiang, J., & Belu, R. (2012). Sub-kilometer dynamical downscaling of near-surface winds in complex terrain using WRF and MM5 mesoscale models. *Journal of Geophysical Research: Atmosphere*, *117*(D11), D11111. https://doi.org/10.1029/2012jd017432

Jiménez, P. A., & Dudhia, J. (2012). Improving the representation of resolved and unresolved topographic effects on surface wind in the WRF model. *Journal of Applied Meteorology and Climatology*, *51*(2), 300–316. https://doi.org/10.1175/jamc-d-11-084.1

Jiménez, P. A., Dudhia, J., González-Rouco, J. F., Navarro, J., Montávez, J. P., & García-Bustamante, E. (2012). A revised scheme for the WRF surface layer formulation. *Monthly Weather Review*, *140*(3), 898–918. https://doi.org/10.1175/mwr-d-11-00056.1

Lee, J., Hong, J., Noh, Y., & Jiménez, P. A. (2020). Implementation of a roughness sublayer parameterization in the Weather Research and Forecasting model (WRF version 3.7. 1) and its evaluation for regional climate simulations. *Geoscientific Model Development*, *13*(2), 521–536. https://doi.org/10.5194/gmd-13-521-2020

Li, M., Zhang, J. A., Matak, L., & Momen, M. (2023). The impacts of adjusting momentum roughness length on strong and weak hurricane forecasts: A comprehensive analysis of weather simulations and observations. *Monthly Weather Review*, *151*(5), 1287–1302. https://doi.org/10.1175/mwr-d-22-0191.1

Liu, Y., Shen, C., Chen, X., Hong, Y., Fan, Q., Chan, P., et al. (2023). Satellite-based estimation of roughness length over vegetated surfaces and its utilization in WRF simulations. *Remote Sensing*, *15*(10), 2686. https://doi.org/10.3390/rs15102686

Maurer, K. D., Hardiman, B. S., Vogel, C. S., & Bohrer, G. (2013). Canopy-structure effects on surface roughness parameters: Observations in a Great Lakes mixed-deciduous forest. *Agricultural and Forest Meteorology*, *177*, 24–34. https://doi.org/10.1016/j.agrformet.2013.04.002

Menut, L. (2018). Modeling of mineral dust emissions with a Weibull wind speed distribution including subgrid-scale orography variance. *Journal of Atmospheric and Oceanic Technology*, *35*(6), 1221–1236. https://doi.org/10.1175/jtech-d-17-0173.1

Moraes, O., Acevedo, O., Degrazia, G., Anfossi, D., Da Silva, R., & Anabor, V. (2005). Surface layer turbulence parameters over a complex terrain. *Atmospheric Environment*, *39*(17), 3103–3112. https://doi.org/10.1016/j.atmosenv.2005.01.046

Nelli, N. R., Temimi, M., Fonseca, R. M., Weston, M. J., Thota, M. S., Valappil, V. K., et al. (2020). Impact of roughness length on WRF simulated land-atmosphere interactions over a hyper-arid region. *Earth and Space Science*, *7*(6), e2020EA001165. https://doi.org/10.1029/2020ea001165

Paulot, F., Naik, V., & W. Horowitz, L. (2022). Reduction in near-surface wind speeds with increasing CO_2 may worsen winter air quality in the Indo-Gangetic Plain. *Geophysical Research Letters*, *49*(18), e2022GL099039. https://doi.org/10.1029/2022gl099039

Prein, A., Ge, M., Valle, A., Wang, D., & Giangrande, S. (2022). Towards a unified setup to simulate mid-latitude and tropical mesoscale convective systems at kilometer-scales. *Earth and Space Science*, *9*(8), e2022EA002295. https://doi.org/10.1029/2022ea002295

Prieto-Herráez, D., Frías-Paredes, L., Cascón, J. M., Lagüela-López, S., Gastón-Romeo, M., Asensio-Sevilla, M. I., et al. (2021). Local wind speed forecasting based on WRF-HDWind coupling. *Atmospheric Research*, *248*, 105219. https://doi.org/10.1016/j.atmosres.2020.105219

Raupach, M. R. (1992). Drag and drag partition on rough surfaces. *Boundary-Layer Meteorology*, *60*(4), 375–395. https://doi.org/10.1007/bf00155203

Schaaf, C., & Wang, Z. (2021). MODIS/Terra+Aqua BRDF/Albedo model parameters daily L3 global—500m V061 [Dataset]. *NASA Land Processes Distributed Active Archive Center*. https://doi.org/10.5067/MODIS/MCD43A1.061

Shen, C., Shen, A., Cui, Y., Chen, X., Liu, Y., Fan, Q., et al. (2022). Spatializing the roughness length of heterogeneous urban underlying surfaces to improve the WRF simulation-part 1: A review of morphological methods and model evaluation. *Atmospheric Environment*, *270*, 118874. https://doi.org/10.1016/j.atmosenv.2021.118874

Song, H., Ni, X., Chang, Y., Chappell, A., Zhou, Z., & Liu, B. (2025). Changing aerodynamic roughness in WRF reduces bias and improves accuracy in near-surface wind simulations [Dataset]. *Figshare*. https://doi.org/10.6084/m9.figshare.30662144

Song, H., Wang, K., Zhang, Y., Hong, C., & Zhou, S. (2017). Simulation and evaluation of dust emissions with WRF-Chem (v3. 7.1) and its relationship to the changing climate over East Asia from 1980 to 2015. *Atmospheric Environment*, *167*, 511–522. https://doi.org/10.1016/j.atmosenv.2017.08.051

Vautard, R., Cattiaux, J., Yiou, P., Thépaut, J. N., & Ciais, P. (2010). Northern Hemisphere atmospheric stilling partly attributed to an increase in surface roughness. *Nature Geoscience*, *3*(11), 756–761. https://doi.org/10.1038/ngeo979

Wagenbrenner, N. S., Forthofer, J. M., Lamb, B. K., Shannon, K. S., & Butler, B. W. (2016). Downscaling surface wind predictions from numerical weather prediction models in complex terrain with WindNinja. *Atmospheric Chemistry and Physics*, *16*(8), 5229–5241. https://doi.org/10.5194/acp-16-5229-2016

Wang, H., Han, S., Liu, Y., Yan, J., & Li, L. (2019). Sequence transfer correction algorithm for numerical weather prediction wind speed and its application in a wind power forecasting system. *Applied Energy*, *237*, 1–10. https://doi.org/10.1016/j.apenergy.2018.12.076

Wang, J., Yang, K., Liu, J., Zhou, X., Ma, X., Tang, W., et al. (2025). Improvement of near-surface wind speed modeling through refined aerodynamic roughness length in built-up regions: Implementation and validation in the Weather Research and Forecasting (WRF) model version 4.0. *EGUsphere*. https://doi.org/10.5194/egusphere-2025-1513

Xu, Z. Q., Xue, T., Chen, X. Y., Feng, J., Zhang, G. W., Wang, C., et al. (2025). Wind power correction model designed by the quantitative assessment for the impacts of forecasted wind speed error. *Advances in Climate Change Research*, *16*(1), 73–81. https://doi.org/10.1016/j.accre.2024.12.006

Yu, E., Bai, R. L., Chen, X., & Shao, L. (2022). Impact of physical parameterizations on wind simulation with WRF V3.9.1.1 under stable conditions at planetary boundary layer gray-zone resolution: A case study over the coastal regions of North China. *Geoscientific Model Development*, *15*(21), 8111–8134. https://doi.org/10.5194/gmd-15-8111-2022

Zhou, Z., Zhang, C., Chappell, A., Zou, X., Zhang, Z., Zuo, X., et al. (2024). Using field measurements across land cover types to evaluate albedo-based wind friction velocity and estimate sediment transport. *Journal of Geophysical Research: Atmospheres*, *129*(4), e2023JD040313. https://doi.org/10.1029/2023jd040313